

BEAM DYNAMICS IN POSITRON INJECTOR SYSTEMS FOR THE NEXT GENERATION B-FACTORIES

N. Iida*, H. Ikeda, T. Kamitani, M. Kikuchi, K. Oide, and D. Zhou
 KEK, 1-1 Oho, Tsukuba, Ibaraki, 305-0801, Japan

Abstract

SuperB and SuperKEKB are the next-generation B-factories, aiming to boost their luminosities to around $10^{36}\text{cm}^{-2}\text{s}^{-1}$. To achieve their goals, high charge and small emittance are required for the injected beams. For the positron beam, it is indispensable to introduce a damping ring (DR). This paper will point out various issues in three sections: for the high emittance beam before the DR, the damping performance in the DR, and the transportation of the small emittance beam after the DR through the injection to the main ring. We will mainly discuss on the issues for the SuperKEKB as a typical case.

INTRODUCTION

The two next generation B-factories[1], SuperB in Italy and SuperKEKB in Japan, aim to increase the peak luminosities to around $10^{36}\text{cm}^{-2}\text{s}^{-1}$. The parameters of the positron collider rings as well as those of the injected beam are listed in Table 1.

Table 1: Parameters of the positron collider rings relevant to (a) the injection and (b) the injected beam

(a) Parameters of Collider ring	unit	SuperB	SuperKEKB	KEKB
Energy	GeV	6.7	4.0	3.5
Stored beam current	A	1.892	3.6	< 1.8
Number of bunches		978	2500	1580
Circumference	km	1.2584	3.016	3
Beam lifetime at collision	sec.	254	340	> 6000

(b) Parameters of injection beam	unit	SuperB	SuperKEKB	KEKB
Charge/bunch required from main ring	nC	0.65	2.1	0.15
Charge/bunch deliverable by injector	nC	0.5 – 2.0	4.0 (Max. 8.0)	1.0
bunch/pulse		1 (Max. 5)	2	2
Maximum total repetition rate	Hz	100	50	50
Horizontal emittance (ex)	nm	4.1	12.5	300
Vertical emittance (ey) (k: X-Y coupling in the damping ring)	nm	0.72 (k = 1%)	0.26 (k = 0%) 0.58 (k = 5%)	200

As the both machines assume a top-up injection, the minimum amount of charge of the injected beam is determined by stored current, circumference, number of bunches, and beam lifetime at collision. On the other hand, even higher charge will be favorable to reduce the refilling time from scratch. In the case of SuperKEKB, while the minimum injected charge per bunch to compensate the lifetime is 2.1 nC, the standard and the maximum charges have been chosen to 4 nC and 8 nC, respectively.

Since both machines are based on so-called “nano-beam” scheme, which has a small dynamic aperture, a very low emittance is required for injected beam.

* naoko.iida@kek.jp

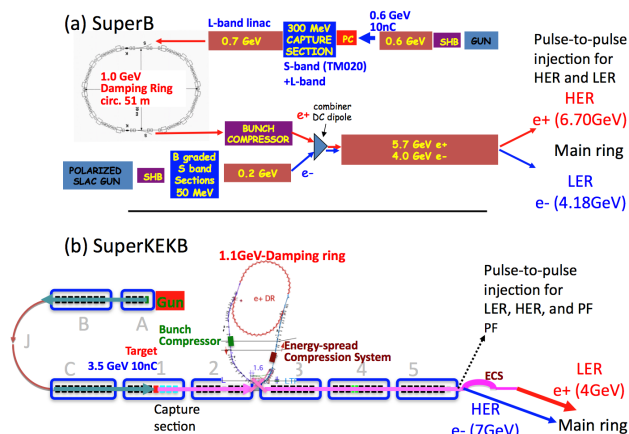


Figure 1: Positron injector complexes: (a) SuperB[2], (b) SuperKEKB[3, 4].

Table 2: Parameters of positron injector

Parameters of Positron Injector	Unit	SuperB	SuperKEKB
Primary electron charge/bunch	nC	10	10
Primary electron energy	GeV	0.6	3.5
Linac frequency before DR	MHz	L-band(TM020) 1428	S-band 2856
Energy compressor before DR		NO	YES
Energy of DR	GeV	1.0	1.1
Bunch compressor after DR		YES	YES
Linac frequency after DR		C-band	S-band
Pulse-to-pulse injection (Particle: Energy)	GeV	HER (e+: 6.7) +LER (e-: 4.18)	LER (e+:4.0)+HER (e-:7.0) +PF (e-:2.5)

The positron injector complexes of the B-factories are shown in Fig. 1. The parameters of the injectors are summarized in Table 2. SuperB has no energy compressor before the DR, because almost all the accelerating structures consist of L-band. For the sake of the long RF wavelength, the resulted energy spread is not so large and acceptable to the DR.

Parameters of injected beam of the DR and those of DR are summarized in Table 3. As shown in Table 3(a), maximizing the captured positrons after the target, emittance and the energy spread becomes enormous. As listed in Table 3(b), while the emittance and the energy spread shrink at the extraction from DR, the resulted bunch lengths remain longer to be accepted by the following linac. The bunch length becomes even longer by the microwave instability due to coherent synchrotron radiation (CSR) in the DR, which will be mentioned in the later section. After the DR, a mission is to transport such a high intensity beam without emittance growth and beam loss, which are more or less common problems for the two B-factory machines.

The common issues for the positron beam are: (1) in the area from positron target to DR, a large amount of charge,

Table 3: Parameters of (a) the injected beam for the DR and (b) the DR

(a) Parameters of injection beam for damping ring	Unit	SuperB	SuperKEKB
Charge (Maximum)	nC	2.0	8
Injected beam emittance	nm	1100	1400
Energy spread	%	1.5	5.0 → 1.5 (w ECS)
(b) Parameters of damping ring	Unit	SuperB	SuperKEKB
Circumference	m	51.1	135.5
Equilibrium horizontal emittance	nm	23	42.0
Equilibrium vertical emittance	nm	0.2(k=0.01)	0.95(k=0)/2.10(k=0.05)
Betatron damping time	ms	7.3	10.9
Momentum compaction		5.7×10^{-3}	1.41×10^{-2}
RF voltage	MV	0.5	1.4
Bucket height	%	2.5	1.5
Equilibrium energy spread		6.2×10^{-4}	5.5×10^{-4}
Bunch length (low current)	mm	4.8	6.6 / 8.4 (for 8nC)

huge emittances and energy spread will cause the serious beam loss. (2) in the DR, microwave instabilities due to CSR will be an issue because the large aperture of the beam pipe is necessary for capturing the large emittance of the injected beam. (3) in the transport from DR to the main ring, preservation of the emittance is vitally important.

In this paper, these issues are investigated making use of tracking simulations[5] from the positron generation through the injection into the collider ring, taking SuperKEKB as a typical example. In SuperKEKB, the amount of beam loss is severely restricted in the DR and the linac-to-collider beam transport (BT) line, whose tunnels are relatively shallow.

FROM POSITRON TARGET TO DR

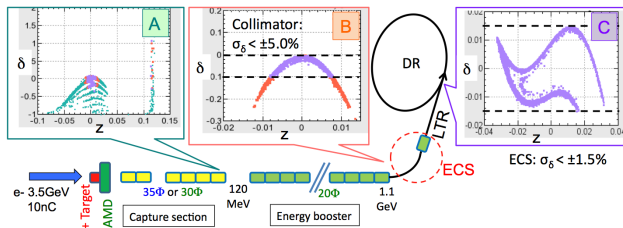


Figure 2: The schematic layout of the system from the positron target to the DR with distributions in the longitudinal phase space: [A] at the end of the capture section, [B] at the extraction point from linac, and [C] at the entrance of DR.

Figure 2 shows the schematic layout of the system from the positron target to the DR for SuperKEKB. The energy and charge of the primary electron beam are 3.5 GeV and 10 nC. The positron target is made of a 14 mm-thick-Tungsten block. The point in the design of the positron capture section is to increase the capture efficiency by enlarging the energy acceptance and also the transverse acceptance. For the energy acceptance, an adiabatic matching device (AMD) is used, which, however, results in a long energy-tail in the lower energy. In SuperKEKB, a flux concentrator is the first candidate for the AMD at present. For the transverse acceptance, acceleration structures with large aperture are needed. An *L-band* structure is the best

solution, while a *Large-aperture S-band* is another option, which will be discussed in the next section. The subsequent linac with S-band structures boost positrons from 120 MeV to 1.1 GeV, then the beam is extracted and transferred to the DR through the linac-to-ring beam transport line (LTR). Owing to the large transverse acceptance of the linac, the emittance before the DR amounts to 1400 nm. The distributions in the longitudinal phase spaces are also shown in the upper part of the Fig. 2. Since the energy spread, especially its low-energy tail, is very large compared to the acceptance of the DR, which is $\pm 1.5\%$, it is important to cut the tail and to compress the energy spread prior to injection to the DR. An energy compression system (ECS) is incorporated in the LTR. Collimators play an important role to prevent the beam loss in the DR. Cutting the energy tail by collimators, the energy spread becomes $\pm 5.0\%$ at the entrance of the ECS. The ECS compresses the energy spread to $\pm 1.5\%$ with 41 MV S-band voltage and $R_{56} = -0.61$ m.

Simulation study has been performed using various codes; EGS4 for the positron generation, a newly developed code by T. Kamitani for the capture process in the capture-section, and SAD[6] for the acceleration and beam transport.

As for the capture-process there are two major points in the design: one is the phase of the RF (acceleration or deceleration), and the other is the acceleration frequency (*L-band* or *Large-aperture-S-band*).

RF Phase of the Capture Section

The energy spread of the positrons right after the target is very broad. In the “acceleration phase”, the generated positrons move on a crest of RF wave, and accelerated normally. In the case of a “deceleration phase”, the positrons are once decelerated to almost zero velocity, caught up by the next RF wave, and accelerated again. The particles in the higher energy tail, on the other hand, taking longer time to be decelerated, catching up the next RF wave with later timing, gains lower energy than the center particles do. Figure 3 illustrates the difference between them. In the acceleration phase there are tail particles at the higher energy at the entrance of LTR (1). Even if the collimators cut the

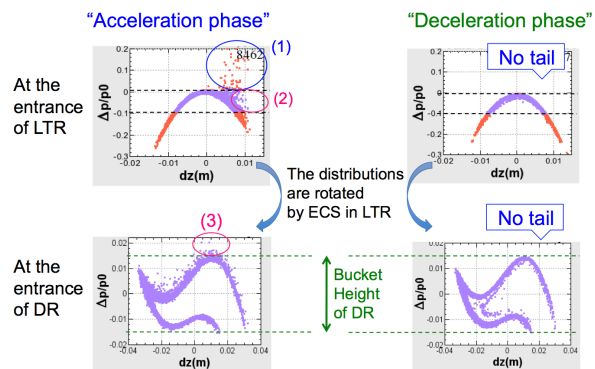


Figure 3: Comparison of longitudinal phase space for the acceleration case(left) and the deceleration (right). The upper (lower) figures show the distributions at the entrance of LTR (DR).

tail at the LTR, there could still exist the other tail in the positive z -direction (2). After rotation in the longitudinal phase space by the ECS, the tail at the z -direction emerges as a new high-energy tail, which is no longer trimmed because no high-dispersion section exists after the ECS (3). In the deceleration phase, however, there is no tail in the energy direction nor z -direction at the entrance of LTR, all positrons after the collimators are injected within the acceptance of DR[7].

While the intensity of the positrons injected to the DR has no significant difference between the acceleration and the deceleration phases (about 6 nC), we have chosen the deceleration phase considering the energy tail.

Accelerating Structure of the Capture Section

Larger apertures of the capture section is obviously better to capture more positrons. From this viewpoint, an L-band structure with a large aperture of $35\text{mm}\phi$, is the best solution, but, considering costs, an S-band structure with large-aperture, say, $30\text{mm}\phi$, might be a candidate. Tracking simulations show that the charges that reach the DR are comparable for L-band and S-band, 6.6 nC and 6.3 nC, respectively.

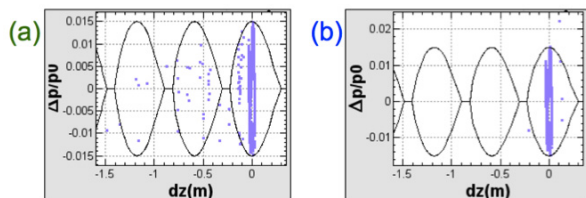


Figure 4: Distributions in the longitudinal phase space for the case of (a) all S-band, and (b) a combination of L-band and S-band.

As shown in Fig. 4(a), for the S-band's, satellite bunches are generated due to the stem from circuitous trajectories by the solenoid field in the capture section. These satellites could cause a beam loss in the DR after injection. As we have to reuse the existing S-band linac as much as possible, the downstream accelerating structures must be S-band. In the L-band case, by choosing a coprime (5:11) frequency ratio of L-band to S-band, 1298 MHz to 2856 MHz, most of the L-band satellites drop into deceleration phase of the following S-band or less accelerated, and are eliminated by the physical aperture of the structure (See Fig. 4(b).) at the end. The beam loss ratio in the DR is estimated as 0.403% and 0.053% for S-band and L-band, respectively. Since the allowable loss rate is less than 0.1% in the case of SuperKEKB-DR, the use of L-band is inevitable.

DAMPING RING

The normal cell of the damping ring[8] is a reversed-bend FODO cell which features a low momentum compaction factor and the dynamic apertures in both of the momentum and transverse direction in general. We have found that the microwave instability due to CSR[9] in the

05 Beam Dynamics and Electromagnetic Fields

D01 Beam Optics - Lattices, Correction Schemes, Transport

DR enlarges the longitudinal emittance. To suppress the instability, the parameters of the DR were changed as: (1) the beam energy was changed from 1.0 GeV to 1.1 GeV, (2) the momentum compaction factor was changed from 0.0019 to 0.0141, (3) the cavity voltage was increased from 0.261 MV to 1.4 MV to obtain higher synchrotron tune, (4) the vertical aperture of vacuum chambers was reduced from 34 mm to 24 mm. The wake potential of CSR is larger than those of ordinal vacuum components in two orders of magnitude even after these changes.

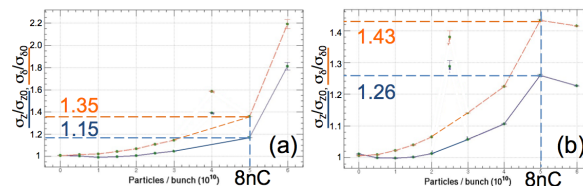


Figure 5: Beam blowup in the longitudinal phase space as a function of the number of positrons per bunch. The results depend on the initial distribution of the bunch: (a) the Hassinski solution, (b) the beam injected from linac.

The enlargements of the bunch length and energy spread due to CSR are estimated by a tracking simulation, in which 5 million macro particles are used. For the initial condition, two types of distributions are prepared. One is a damped beam whose distribution in the longitudinal phase space obeys Gaussian. Another is an undamped beam which are generated by a tracking simulation from the target to the DR, whose distribution is shown in the Fig. 2[C]. The result differs between the two cases. The growth rate for the case of undamped beam(b) is higher than that of damped beam(a). The two initial beams are different not only in the longitudinal distribution but also in the energy distribution. The beam from the linac has larger energy spread in one order of magnitude. The quasi-equilibrium state depends on the initial beam distribution, not on the spreads of the energy.

We have found that around a specific bunch intensity in Figs. 5(a) and (b), a high-frequency instability appears. In these very narrow region of the bunch intensity, the particles in the longitudinal phase space excite a high-frequency modulation at $k \sim 4\pi/\sigma_z$ to enlarge the emittance as shown in Fig. 6.

The microwave instability due to CSR could be a common issue to damping rings with a high bunch-current and

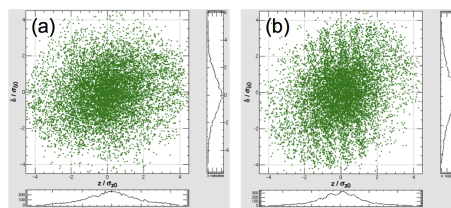


Figure 6: The distribution of particles in the longitudinal phase space where a high-frequency instability is seen. Only 10,000 particles are shown out of 5,000,000 tracked particles. At this intensity, the density modulation alternates between (a) weak and (b) strong with a period of about 4,000 turns.

a low emittance. For the positron, in order to obtain a high bunch-charge, the emittance from positron production system tends to be large, and the physical aperture of DR needs to be large, which results in the intense microwave instability due to CSR. The issues of microwave instability caused by CSR may affect the design of damping rings for SuperB, ILC, CLIC, etc.

FROM DR TO MAIN RING

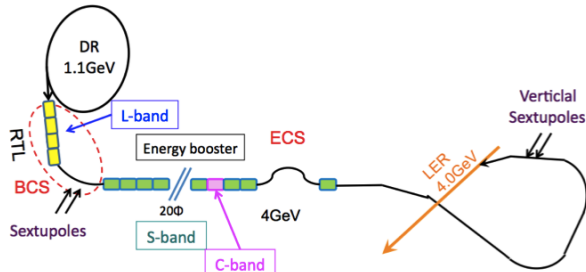


Figure 7: A schematic layout of the linac and the beam transport lines from the DR to the main ring.

Figure 7 shows a layout of the linac and beam transport lines from the DR to the main ring. The extracted beam must be transported to the entrance of the main ring preserving the emittance. After the DR, The bunch length is reduced by one order of magnitude through a bunch compression system (BCS) to cope with the RF curvature of the downstream linac where the S-band and a few C-band structures are used. We should use L-band accelerator structures for the BCS to match the long bunch-length. There is another ECS at the end of linac in order to match the beam with the momentum acceptance of the main ring.

Transporting the high bunch-intensity of 8 nC after the DR, various sources of emittance growth are considered :
 1. Enlargement of the energy spread; 2. The transverse emittances blowup due to (1) misalignments of accelerating structures as well as quadrupoles, (2) second-order dispersion in the transport lines, (3) synchrotron radiation in the transport line, (4) beam-beam effect after injection into the main ring (LER).

Enlargement of the Energy Spread

In acceleration of high bunch-intensity of 8 nC, a strong wake field of accelerating structure has a sizable effect on the beam. To simulate the effects, a wake potential by Yokoya's approximated formula[10] is included in our simulation. The RF-phase at three parts of accelerating structures should be adjusted, which is the same process in the actual beam operation; (a) L-band in the BCS, (b) S-band and C-band in the linac, and (c) S-band in the ECS at the end of linac are shown in Fig. 7.

Figure 8 shows the optimization results of the acceleration phases to minimize the energy spreads. The bunch length dependence on the phase fits well with parabola except at the bottom in Fig. 8(c), which is a manifestation of the non-Gaussian distribution. The widths of energy- and bunch-length are $\pm 0.271\%$ and $\pm 21.9\text{ mm}$, which are in

Tuning knob	L-band of BCS	S,C-band in LINAC	S-band of ECS	
Place	Entrance of LINAC	End of LINAC	Exit of ECS	Entrance of main ring
σ_z [mm]	± 0.896	± 2.15 (99% incl.)	± 10.87 (99% incl.)	± 21.93 (99% incl.)
σ_δ [%]	± 0.825	± 1.13 (99% incl.)	± 0.271 (99% incl.)	± 0.271 (99% incl.)

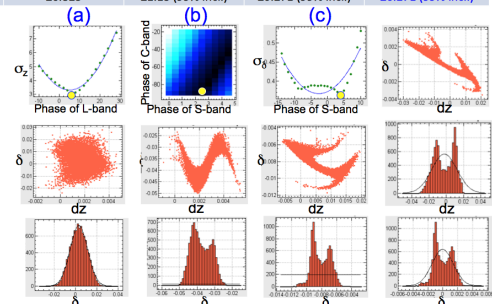


Figure 8: Optimization of acceleration phase to minimize the energy spread

the acceptable level for injection to LER. By these careful adjustments, almost 100 % of transmission efficiency can be achieved.

Transverse Emittance Growth

Misalignments The misalignments of accelerating structures and quadrupoles cause the transverse instability due to the transverse wake field. In the simulation it is assumed that the accelerating structures and the quadrupoles have random lateral misalignments with Gaussian distribution. The orbit distortion are corrected by corrector magnets.

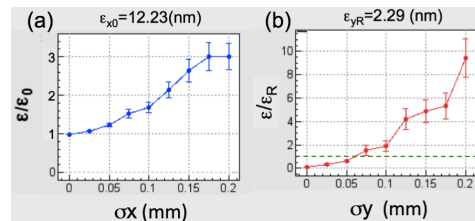


Figure 9: Emittance growth at the entrance of LER as a function of misalignment-amplitude. (a) Horizontal emittance growth, (b) Vertical emittance growth for injection to the LER. The green line shows the allowable level for injection to LER.

Figure 9 shows the emittance-growth dependence on the misalignment amplitude. The horizontal blowup is not a serious issue to the injection because the horizontal injection amplitude is dominated by the thickness of a injection septum. The vertical blowup in Fig. 9(b) has more serious consequences. In order to suppress the growth within the vertical acceptance for injection, misalignments should be confined within $60\ \mu\text{m}$, which is a very tight tolerance. Good news is that those emittance growths due to the transverse wake effect can be cancelled in some level, by properly choosing the initial offset and angle of the orbit at the entrance of linac[11].

Second-order Dispersion The energy spread of the beam is $\pm 1.9\%$ after the BCS of the extraction line from DR to linac (RTL), and $\pm 0.27\%$ at the BT to LER, where we define the spread as the width that contains 99 % of particles. In these regions, the emittance growth due to the second order dispersion is not negligible. As shown in

Fig. 10, the transverse positions and momenta are distorted at larger energy offset without the sextupole correction. Emittances without/with sextupoles are 45.9/40.2 (nm) and 0.351/0.269 (nm) at the end of RTL and BT, respectively. No emittance growth is observed after the corrections.

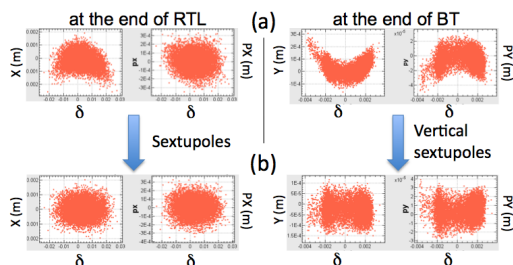


Figure 10: Correction of the second order dispersion using sextupoles. The left and right graphs show corrections at the end of RTL and BT. The figures show correlation plots of the transverse position and transverse momentum versus energy deviation for the case (a) without sextupoles, (b) with sextupoles.

Synchrotron Radiation in the BT The emittance growth due to the synchrotron radiation in the transport line between linac and LER is not negligible because the emittance itself is very small. The growth factor by this effect is only 13 % in the horizontal plane and almost no growth in the vertical. This effect is not an issue for the injection.

INJECTION INTO THE MAIN RING

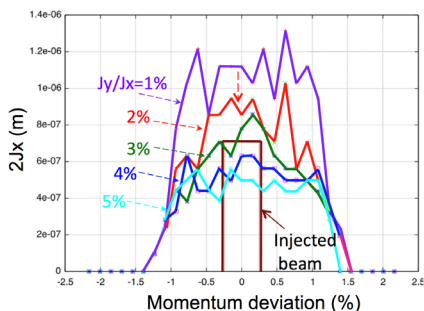


Figure 11: Dependence of dynamic aperture of the main ring on the vertical action of the injection beam. The horizontal axis is the momentum deviation and the vertical is the horizontal injection aperture. J_y/J_x is the ratio of the vertical action to the horizontal one of the injected beam. The rectangle region corresponds to the injected beam discussed so far.

The maximum horizontal-action and the energy deviation of injected beam are drawn as a rectangle in Fig. 11, using the simulation results. If J_y/J_x of the injected beam is less than 2%, which corresponds to the vertical action of 7 nm, it is within the dynamic aperture. In this case the vertical emittance necessary to transmit 95.5% assuming Gaussian is 2.29 nm. On the other hand, the vertical emittance assuming 5% coupling in the DR is 0.58 nm, which is well below the required value.

Beam-beam Effect The last issue is the vertical emittance growth due to beam-beam effect. By the beam-beam kick from the stored beam, the vertical emittance of the injected beam is transiently grown 16 times larger than that

without beam-beam effect. That is caused by the vertical incoherent motion. This is especially strong in the nano-beam scheme, where the vertical beta function has very small waist at the interaction point. The particle with a large horizontal position and with nonzero vertical offset receives a beam-beam kick at the location that has a very large β_y . Due to the effect, 5.5 % beam particles are estimated to be lost in the main ring. This effect is under investigation.

SUMMARY

We have investigated the positron injector systems for the next-generation B-factories making use of a particle tracking simulation from the positron target to the injection to the collider ring. The issues in the three sections of the injector complex have been discussed as:

1. From the positron target to the DR, transporting the large emittance beam without beam loss is resolved by choosing a proper acceleration schemes, including the combination of RF frequencies in the capture section and in the linac.
2. In the DR, longitudinal emittance growth caused by microwave instability due to coherent synchrotron radiation, is mitigated by a smaller height of the beam pipe, a larger momentum compaction factor, and a higher synchrotron tune.
3. From the DR to the main ring, issues are expected including transverse beam breakup, longitudinal gymnastics, higher order dispersions/chromaticities, synchrotron radiation, and the beam-beam effect at the injection. We have shown some mitigation techniques for each issue.

The issues inherent in the the positron injector systems of the next-generation B-factories, could be also relevant to other positron injectors including the ILC, CLIC, etc.

ACKNOWLEDGEMENTS

Authors would like to thank S. Guiducci and A. Variola of the SuperB Group for providing the information.

REFERENCES

- [1] H. Koiso *et al.*, IPAC2011, FRXBMH01
- [2] S. Guiducci and A. Variola, private communication, IPAC2011, THPZ024, and the SuperB Collab. at Elba 2011, <http://agenda.infn.it/conferenceDisplay.py?confId=3352>
- [3] T. Kamitani *et al.*, LINAC2010, Tsukuba, Japan, p.70.
- [4] M. Satoh *et al.*, LINAC2010, Tsukuba, Japan, p.703.
- [5] N. Iida *et al.*, IPAC2010, THPD004
- [6] <http://acc-physics.kek.jp/SAD/sad.html>
- [7] http://research.kek.jp/people/iida/THYA01_talk_movie.ppt
- [8] M. Kikuchi *et al.*, IPAC2010, TUPEB054
- [9] H. Ikeda, et al. *et al.*, IPAC2011, THPZ021
- [10] K. Yokoya, private communication.
- [11] L. Zang *et al.*, IPAC2011, MOPS058